Journal of Physics: Conference Series

PAPER • **OPEN ACCESS**

Silicon nanoparticles as active materials for LED: laser synthesis and functionalization for tuning luminescence

To cite this article: R. D'Amato *et al* 2022 *J. Phys.: Conf. Ser.* **2315** 012002

View the article online for updates and enhancements.

You may also like

- Confined silicon nanospheres by biomass lignin for stable lithium ion battery
Xiaoying Niu, Jinqiu Zhou, Tao Qian et al.
- Large-scale high-quality 2D silica crystals: dip-drawing formation and decoration with gold nanorods and nanospheres for SERS analysis
Vitaly Khanadeev, Boris N Khlebtsov, Svetlana A Klimova et al.
- Nonthermal plasma synthesis of silicon nanoparticles and their thermal transport properties
Firman Bagja Juangsa, Meguya Ryu, Junko Morikawa et al.

This content was downloaded from IP address 192.107.67.240 on 27/10/2023 at 16:00

Silicon nanoparticles as active materials for LED: laser synthesis and functionalization for tuning luminescence

R. D'Amato[1], S. Dello Iacono[1,2], A. Santoni[1], P. Reale[1], F. Limosani[1], G. Terranova[1], S. Botti[1], F. Bonfigli[1], A. Migliori[3], S. Scalbi[4]

[1]Photonics Micro and Nanostructures Laboratory, Fusion and Technologies for Nuclear Safety and Security Department, Physical Technologies for Safety and Health Division, ENEA, C.R. Frascati, Italy
[2]Institute of Applied Sciences & Intelligent System "Eduardo Caianiello" (ISASI), CNR, Napoli, Italy
[3]Institute for microelectronics and microsystems (IMM), CNR, Bologna, Italy
[4] Laboratory Resources valorization, Department for Sustainability, Division Resource Efficiency, ENEA C.R. Bologna, Italy

E-mail: rosaria.damato@enea.it

Abstract. Silicon nanocrystals (SiNPs) are an extensively studied light-emitting material due to their inherent biocompatibility and easy integration with silicon-based technology. Although low luminescence quantum yields of as-prepared SiNPs, the exploitation of the surface chemistry of SiNPs plays a key role in tuning their luminescence. In this work, the development of SiNPs as active materials for innovative LEDs was investigated. SiNPs were synthesized by using laser pyrolysis, a very flexible tool for lab-scale production in developmental quantities. The synthesized SiNPs have dimensions from 5 to 15 nm and high purity grade but show weak luminescence. For this reason, chemical treatments were performed on SiNPs: surface modifications lead to an improvement of their luminescence properties. Chemical and optical characterization were performed by conventional and advanced techniques, such as FTIR, BET, UV-VIS absorption and emission, XPS, TEM and confocal Raman. A Life Cycle Assessment (LCA) study of laser synthesis of SiNPs was conducted with the aim to identify the potential environmental impacts coming from this production method.

1. Introduction

Semiconductor nanoparticles (NPs) have received widespread attention in recent years for their sizetunable ultraviolet-to-near infrared light emission governed by the quantum confinement effect [1]. The photoluminescent particles, with size-tunable, narrow emission and broad absorption spectra, have been exploited in numerous applications, including in light-emitting/harvesting devices and for biomedical tracking and imaging. Although predominantly, direct band gap semiconductor NPs, *i.e.*, quantum dots (QDs), have thrived in semiconductor NP synthesis and application studies, attention has more recently turned toward the development of potentially less toxic, particularly relative to II–VI Cd- and Pb-based QDs, SiNP fluorophores.

Silicon is inert, nontoxic, abundant, low-cost, biocompatible, and widely used in microelectronics. Si nanostructures are arguably the most attractive and important material in nanoscience and

Content from this work may be used under the terms of the Creative Commons Attribution 3.0 licence. Any further distribution of this work must maintain attribution to the author(s) and the title of the work, journal citation and DOI.
Published under licence by IOP Publishing Ltd

nanotechnology. Although photoluminescent SiNPs are considered biologically advantageous compared to II−VI QDs due to their lower cytotoxicity [2], controlling over the emission characteristics of colloidal Si NPs is relatively challenging. Particularly, the emission λ_{max} is not always correlated with particle size, an expectation of quantum confinement, and the emission λ_{max} can furthermore change with respect to time and chemical environment. The origin of light emission for nm-sized Si domains, whether in colloidal SiNPs (*i.e.*, free-standing) or in SiNPs embedded in solid hosts (e.g., nanocrystalline Si domains in porous Si), has been the subject of intense debate since the observation of efficient, visible light emission from crystalline, nanometer-sized Si domains over two decades ago [3]. While SiNPs prepared by some methods have emission maxima well correlated with particle size [4-6], as expected for an emission process strictly governed by quantum confinement, other reports show particle size distributions and emission spectra not according to expectations of the quantum confinement theory [7]. Several recent reports on the origins of SiNPs photoluminescence (PL) agree that both core and surface states may give rise to visible light emission [8-11], although there is still variation in assignments of size-dependent core *vs* (presumably) size-independent surface states.

Life cycle assessment (LCA) is a standard method regulated by the international standards ISO 14040- 14044:2020 [12, 13], recently amended, and permits to evaluate the environmental impact of processes and products. In literature, there are several applications of the LCA on nanoproducts and nanotechnologies to understand the environmental impacts and/or to highlight possible improvement in production and/or use [14].

In this work, the development of SiNPs as the active materials for innovative LEDs was studied, exploiting the key role of NPs surface chemistry in the tuning of luminescence. SiNPs were synthesized by using laser pyrolysis, a very flexible tool for a lab-scale production. Chemical treatments were performed on SiNPs: surface modifications of NPs lead to an improvement of their luminescence properties. Chemical and optical characterization of the nanoparticles were performed by conventional and advanced techniques, such as FTIR, BET, UV-VIS absorption and photoluminescence (PL), XPS, TEM, confocal Raman. A LCA study of laser synthesis of SiNPs was performed with the aim to identify which are the most environmental impacts phase in the production.

2. Experimental

All the chemicals were analytical grade purchased by Sigma-Aldrich and used as received: hydrofluoric acid (aqueous HF, 49% wt.), ethanol (C_2H_6O, anhydrous), pentane (C_5H_{12}, anhydrous), 1-decene ($CH_3(CH_2)_7CH=CH_2$, 99%), 1-octadecene ($CH_3(CH_2)_{15}CH=CH_2$, 99%), toluene (C_7H_8, 99%).

SiNPs were synthesized by CO_2 laser-driven pyrolysis process in a continuous gas flow reactor, using silane as gas precursor. The experimental set-up and the specific procedure for laser synthesis were described in detail elsewhere [15]. Briefly, the continuous wave (CW) CO_2 laser beam (λ = 10.6 μm) is focused by a spherical lens (focal length F.L. = 19 cm) at the center of the reaction chamber (volume V $\sim 6.8\times10^{-3} m^3$) where it orthogonally intersects the reactant gas flow. The maximum laser power is 1.2 kW and the power density in the focal region can be varied up to 275 kW/cm^2. Reactant gases enter the chamber through the inner tube of a coaxial stainless steel nozzle. Ar flows through the outer tube with the purpose of confining and cooling the particles. The pressure in the reaction chamber is kept constant and measured by a pressure control unit.

BET measurements were carried by using Monosorb (Quantachrome instrument), a single point surface area analyzer.

The IR spectra were performed with FTIR (Fourier Transform InfraRed) spectrophotometer (Shimadzu-IR Affinity-1S) equipped with a single reflection ATR (Attenuated Total Reflectance) diamond cell. The FTIR-ATR needs of minimal sample preparation. The sample is directly in contact with the ATR crystal. The IR radiation cross the crystal and interacts with the sample in contact with the ATR crystal. The measurements, 45 scans for each spectrum (resolution 4 cm^{-1}), were performed at room temperature. The reduction of the IR spectral data (ATR penetration depth compensation, baseline

subtraction and normalization) and the fitting were performed using the Lab solution Shimadzu spectral analysis software, such as the bands deconvolution routine.

UV-Vis absorption measurements were measured using a Jasco V-750 Spectrophotometer in the spectral range of 200-800 nm; PL emission spectra were recorded by a FluoroMax 4 Plus (Horiba) spectrofluorometer in the spectral range from 450 to 700 nm.

The XPS analyses were carried out with a PSP TSX-400 non-monochromatized photon source operated at 1253.6eV (MgKα) and a VG CLAM2 analyzer in an ultra-high-vacuum chamber where base pressure was kept below 5 x 10-10 mbar. Core-level photoemission data were acquired at 50 eV pass energy and 0.1eV step. The spectra were fitted using the CASA XPS software with pseudo-Voigt line shapes.

The Transmission Electron analyses (TEM) were performed with a FEI TECNAI F20 microscope operating at 200 keV. The instrument is also equipped with an energy dispersion X-ray (EDS) and the STEM accessory. The TEM image were taken in the phase contrast mode (HREM). SiNPs dispersion in ethanol was drop-casted on a holey carbon film and dried at 50 °C before the analyses.

Raman spectra and luminescence spectra on powders were recorded by Raman confocal spectrophotometer XpLora Plus Horiba (excitation laser wavelength 532 nm).

An ultrasonic treatment using a high-power ultrasonic probe (Fisherbrand Model 505 sonicator equipped with 3 mm micro-tip probe) was applied on nanoparticles dispersion in ethanol for 30 min to induce disaggregation before PL measurements and for 60 min before chemical functionalization. After ultrasonic treatment, dispersion of SiNPs in ethanol (1g/L) was placed in a Teflon beaker and chemically etched according to a modified literature procedure [16]. Briefly, the chemical etch mixture was prepared by combining aqueous HF, ethanol, and H_2O in a 1:1:1 volume ratio. The chemical etch mixture containing SiNPs was vigorously stirred for 1 h, at ambient temperature. After etching, the HSiNPs underwent biphasic extraction from the aqueous etch mixture using pentane as the apolar phase; these pentane extracts were combined and concentrated. Oxidized SiNPs preferentially partition into water, while H-SiNPs preferentially partition into apolar solvents (where they may subsequently become oxidized over time), so that biphasic extraction assists with isolation of unoxidized, colloidal SiNPs.

Synthetic preparations of the alkyl-terminated SiNPs were performed under inert (N_2) atmosphere using standard air-free techniques. Dispersion of the alkyl-terminated SiNPs was prepared and handled under ambient atmosphere. The SiNPs were functionalized via thermal hydrosilylation reaction [17] of the H-SiNPs with 1-decene and 1-octadecene. In a typical thermal hydrosilylation reaction, 10 mL of degassed 1-decene or 1-octadecene was added into a two-necked round bottom flask containing H-SiNPs (dried after pentane removal under vacuum). The solution was briefly sonicated and subsequently brought to reflux with vigorous stirring for 24 h under inert atmosphere. After cooling to room temperature, the alkyl-terminated SiNPs dispersion was taken to dryness on a rotary evaporator to remove excess, unreacted 1-decene or 1-octadecene. The alkyl terminated SiNPs were then dispersed in 5 mL of dry hexanes or toluene and stored under N_2 for further characterization and use.

3. Laser Synthesis of SiNPs

CO_2 laser pyrolysis of silane (SiH_4) demonstrated its ability to produce light-emitting SiNPs with a very narrow size distribution (in the range of few nanometers), in very small amount. The need of weighable batches of SiNP for different applications has triggered the development of laser pyrolysis method, which is a continuous gas flow process inherently well suited for mass production. Laser pyrolysis is based on the resonance between the emission of a CO_2 laser at 10.6 μm and the absorption of gaseous or liquid precursors. The principle can be briefly described: the SiH_4 gas stream, guided by a coaxial inert gas flow, intersects the laser beam in a reactive chamber under controlled pressure. Provided that the precursor absorbs the infrared laser radiation, the high laser power induces a rapid increase of the temperature in the interaction zone, SiH_4 is dissociated and Si nanoparticles nucleate and grow in this supersaturated phase. A luminescent flame (Figure 1) materializes the reaction. The confinement of the

reactants in an Ar flow avoids any reaction with the reactor walls and though protects the powders from any pollution. The reaction time is very short (0.1–1 ms), since it is controlled by the residence time in the laser beam, which mainly depends itself on the precursors flow and on the nozzle diameter. This time is inherently short and therefore the grain growth is quenched, leading to nanosized particles. Ethylene (C_2H_4) gas is also added to silane as sensitizer, with the purpose of diluting the reactive phase and limit the collisions between radicals in order to inhibit the particle growth, without cooling the gas mixture, but rather contributing to increase the average temperature by coupling the laser energy into the system also at the low concentrations of silane. SiNPs produced in the reaction zone were carried out by the Ar flow and collected in a bag placed downstream in the pumping line.

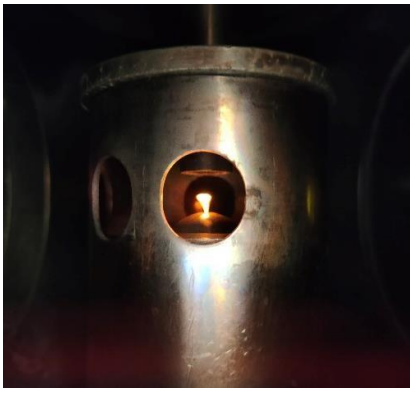

Figure 1. Photo of the flame during SiNPs synthesis

Adjusting process parameters, SiNPs in the range 5–15 nm, different surface characteristics and productivity higher than 1g/h can be obtained in a controlled and reproducible way. In particular, two products are considered for subsequent characterization and functionalization: reaction parameters and main characterization are reported in Table 1.

Table 1. Synthesis parameters. Laser power = 1200 W, Φ (Ar confinement) = 2000 sccm

Samples	P (Pa)	Φ_{SiH4} (sccm)	Φ_{C2H4} (sccm)	Productivity (g/h)	<D> (TEM) nm	□ (TEM) nm	SSA m^2/g	<D> (BET) Nm
SiNP-A	10660	300	100	1,5	14.1	4.0	184.2	14
SiNP-B	8000	250	50	1,1	13.0	6.1	170.2	15

In the reported experiments, the CO_2 laser power is of about 1200 W and the laser beam diameter in the focal region is approximately 5 mm. In order to decrease the residence time of the particles in the reaction zone and limit their growth, the reactor pressure is kept at $8\text{-}11\times10^3$ Pa and Ar flow was 2000 sccm. The silane flow is fixed at 250-300 sccm and ethylene flow is 50-100 sccm.

4. Characterization of SiNPs

The size of dry collected nanoparticles is estimated by adsorption measurements and by High-Resolution Transmission Electron Microscopy (HREM) observations. By the Brunauer, Emmet, Teller (BET) method, specific surface area of the powder is evaluated, and considering spherical particles and assuming theoretical density of Si, particles size is easily deduced. HREM observations permit to see the particle shape, to identify their crystalline state, and to determine their size distribution through statistical analysis.

Figures 2a, 2b present HREM images of the samples showing individual round nanocrystals, surrounded by an amorphous layer of silica, due to the surface oxidation of the nanocrystals exposed to ambient air before observation. Such oxide layer is known to form around SiNPs by a self-limiting process. A simple counting on more than 120 SiNPs indicates for SiNP-A an average diameter of 14.1 nm with a standard deviation of 4.0 nm (DP= 14±1 nm), while for SiNP-B an average diameter of 13.0 nm with a standard deviation of 6.1 nm (DP=13±2 nm) in agreement with BET measurements. These data are summarized in table 1. In Figures 2c, 2d the particle size distributions are reported for the two samples. In laser pyrolysis, the size of produced particles can be controlled by acting on the process parameters, above all on residence time that depends on pressure in the reaction camera. In particular, a larger part of nanoparticles SiNP-B is under 10 nm diameter, and SiNP-B is obtained at lower pressure and at lower concentration of silane.

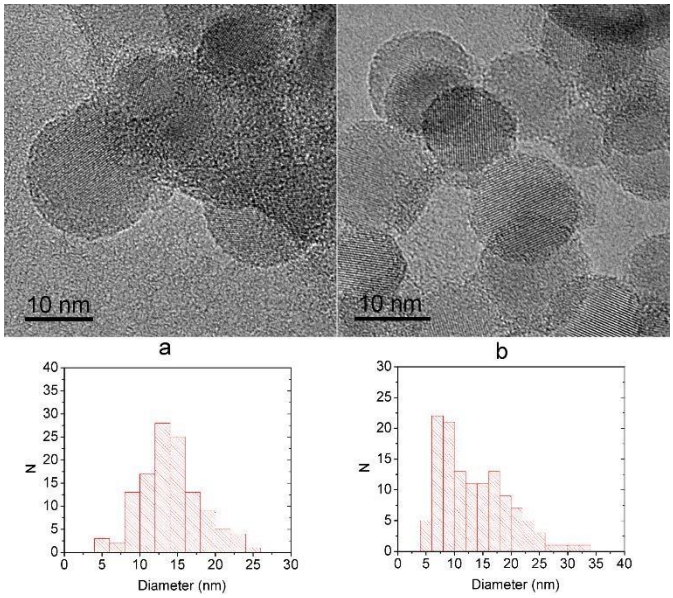

Figure 2. HREM images of SiNP-A (a) and SiNP-B (b). Particle size distribution for SiNP-A (c) and SiNP-B (d)

Moreover, differences between SiNP-A and SiNP-B emerge when we evaluate EDS analysis: in addition to the presence of silicon, as highlighted by the SAEDs, the oxygen peak is detected for both the powders. For SiNP-A a rough estimate of the Si/O ratio is 1:1, while for SiNP-B Si/O ratio is 2:1. Chemical characterization of the nanopowders was obtained by FTIR analysis. In the IR spectra, different chemical characteristics of surfaces, *i.e.* different kind of hydrogenated surfaces, can be observed, while all powders are covered by silicon oxide. The spectra of as-prepared powders show two regions of interest, as illustrated in Figure 3. The first comprises the bands relative to Si-H bonds, at 2250-2100 cm^{-1} that are not strong, giving evidence for not highly hydrogenated surfaces. The second important region is around 1300–800 cm^{-1}, namely in the range typical of Si sub-stoichiometric and stoichiometric oxides, where the band at 1047 cm^{-1} with a shoulder at 1115 cm^{-1} reveals the presence of substoichiometric silicon oxide SiO_x.

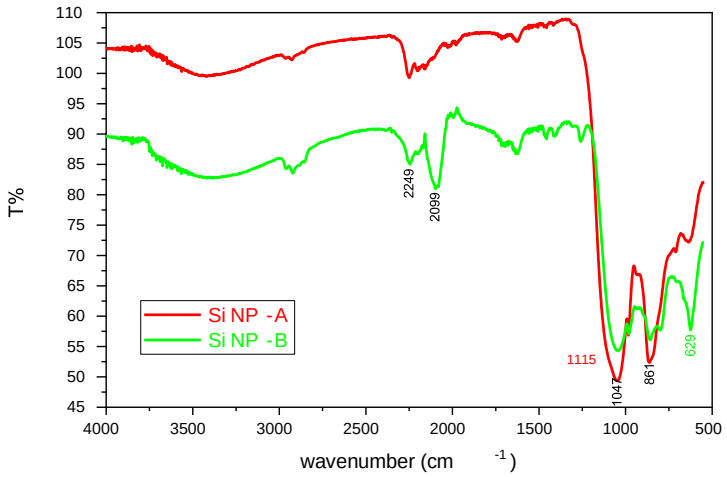

Figure 3. FTIR spectra of SiNP-A (red) and SiNP-B (green).

Raman spectra were performed on powders by using a Raman spectrometer combined with a confocal optical microscope, and mapping of the Raman signals was obtained for both the samples (Figure 4 a, 4c). Raman spectroscopy has the ability to provide a spectroscopic signal sensitive to the size of crystals and their distribution. It is an excellent nondestructive optical technique that probes the phonon density of states and is highly sensitive to crystalline order and symmetry. Raman spectroscopy has been widely used to characterize amorphous and nanocrystalline silicon structures [18, 19]. The transverse-optic (TO) Raman mode that appears at ~520 cm^{-1} in crystalline Si broadens and shifts to lower wavenumbers at ~480 cm^{-1} in case of amorphous silicon.

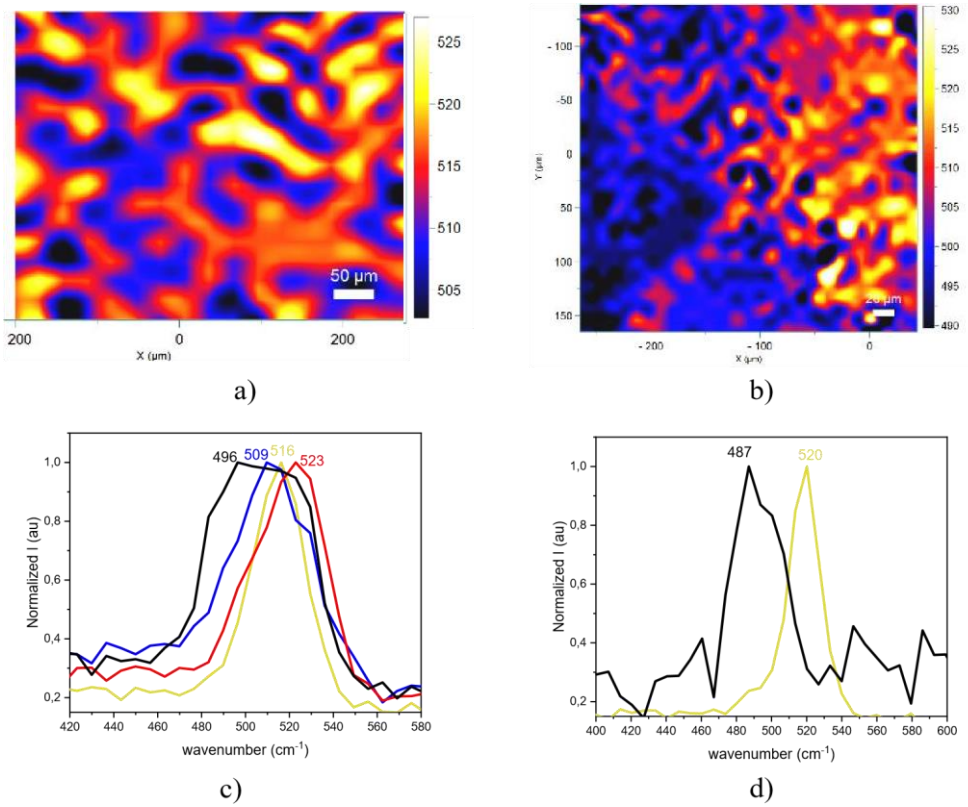

Figure 4. Raman mapping images of SiNP-A (a) and SiNP-B (b). Raman spectra of SiNP-A (c) and SiNP-B (d)

In our cases, spectra are recorded in different points of the powders (Figure 4b, 4d): peaks shape shows that SiNPs were always crystalline, but multiple images point out nanoparticles with different sizes. This is true for both the samples; however, SiNP-B had a larger percentage of nanoparticles under 10 nm, as confirmed by TEM analysis.

Optical characterization of the as-prepared powders was performed. The samples were dispersed in ethanol and stable suspensions were obtained using a high power ultrasonic tip. Absorbance and emission spectra of the solutions were recorded by using a spectrophotometer. Both the samples showed an absorption in the UV region at about 350 nm and a very weak PL emission above 700 nm, in the red region (Figure 5a, 5b).

PL was recorded also by using confocal Raman instrument directly on powders. For these characterizations, PL mapping was performed: SiNP-A shows emission maximum at 690 nm, but spectra with maximum at higher wavelength are also present (Figure 5c); SiNP-B shows unvarying PL and an example is reported, with λ_{max} = 693 nm, in the red region (Figure 5d).

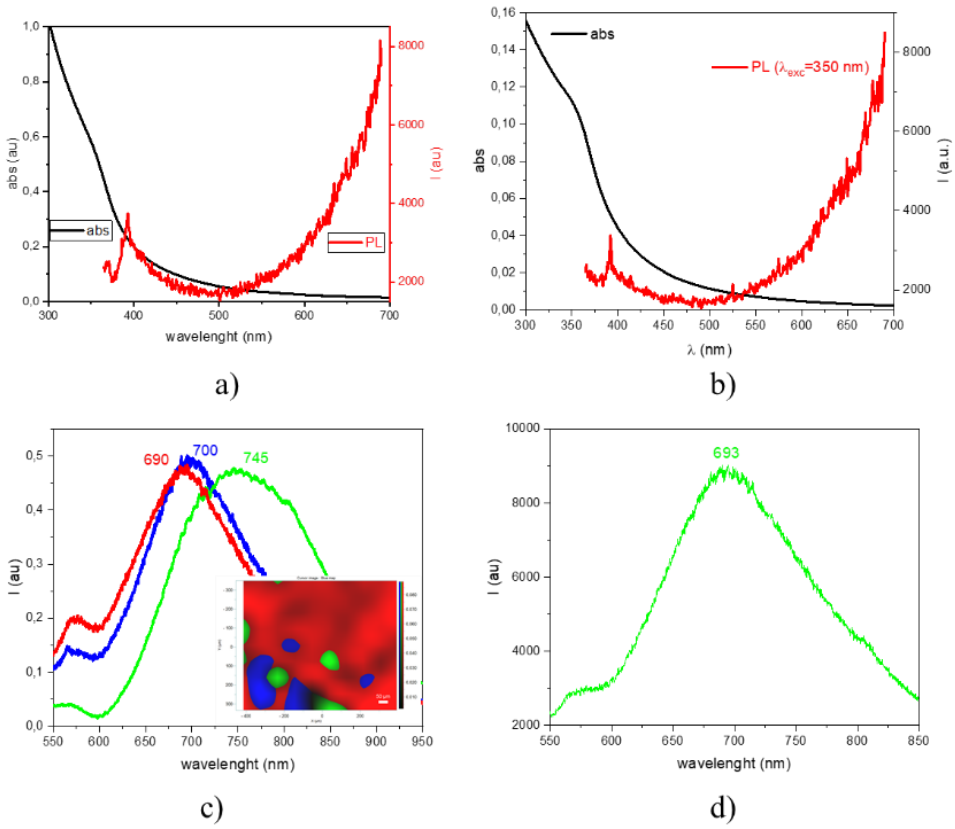

Figure 5. Absorption and emission spectra of powders dispersed in ethanol: SiNP-A (a) and SiNP-B (b). PL spectra of powders SiNP-A (c) and SiNP-B (d). In the inset, mapping of PL for SiNP-A

5. XPS Characterization of SiNPs

A deeper chemical investigation was performed for both the samples by using XPS technique. Figures 6a, 6b show the Si2p photoemission spectra recorded on sample SiNP-A and SiNP-B, respectively.

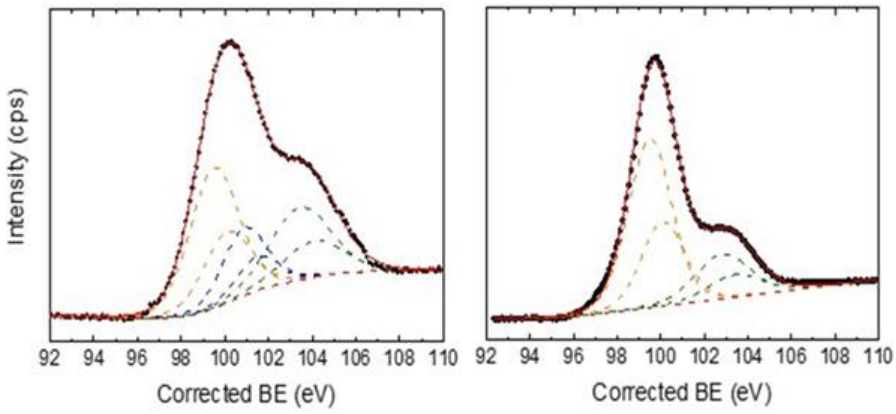

a) b)

Figure 6. Si2p photoemission spectra of sample SiNP-A (a) and SiNP-B (b).

Due to a considerable charging, the raw photoemission data are shifted to higher binding energy and the BE in the figure was corrected by setting Si(0) at 99.5 eV. The SiNP-A and SiNP-B Si2p data were fitted by means of pseudo-Voigt lineshapes in terms of doublets with fixed 0.6 eV spin-orbit separation and 0.5 area ratio. The lineshape appears to be in both cases a convolution of at least two components, due to Si(0) and oxidized silicon. The overall shape of the Si2p spectral intensity shows a peak at lower BE and a bump shifted to higher BE by about 3.5-4 eV in both samples. These two visible features can be indicatively attributed to Si(0) and Si(IV).

The best fit for sample SiNP-A (Figure 6a) shows the presence of three doublets. The lowest BE doublet corresponds to Si(0). The highest BE doublet shifted by 4 eV from Si(0) is assigned to Si(IV) in accord with literature data [20]. According to [20], the suboxides Si(I), Si(II) and Si(III) BE shift is 0.95 eV, 1.75 eV and 2.48 eV, respectively. The intermediate doublet (blue dashed line in Figure 5a) at about 1.40 eV from the main Si(0) is assigned to suboxides, possibly Si^{1+} and/or Si^{2+}. That uncertainty is due to the broadening caused by sample charging, which makes difficult fitting features hidden in the lineshape.

Sample SiNP-B can be fitted by using only two components, i.e. Si(0) and Si(IV), shifted 3.3 eV, nevertheless, bearing in mind the broad lineshapes, the contribution of more silicon oxidation states cannot be excluded.

Comparing the relative intensities of the oxide contributions in the two samples it appears that SiNPA is far more oxidized than SiNP-B, confirming results from EDS analysis.

6. Functionalization of SiNPs

The red-emitting SiNPs used in this study were prepared by alkylic functionalization of nanoparticles surface grafting of organic molecules on SiNPs. High coverage grafting was enabled by use of an etching process that produces a hydrogen-terminated surface on the nanoparticles with very little residual oxygen and by carefully excluding oxygen during grafting reaction. We prepared three samples by reaction of SiNP-A with 1-octadecene (SiNP-A-ODE) and SiNP-B with 1-octadecene (SiNP-B-ODE) and 1-decene (SiNP-B-DEC).

The reaction of the terminal double bond with the reactive Si–Si and Si-H surface radicals results in the formation of covalent Si–C bonds, which are preventing further oxidation of the silicon surface. The Si-H groups can efficiently be activated to hydrosilylation by temperature. The reaction is shown in Figure 7.

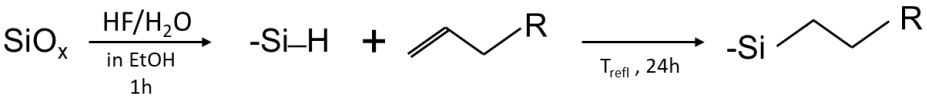

Figure 7. Scheme of the reaction

Grafting of organic molecules onto the SiNPs substantially changes their chemical and physical properties. After reaction, the particles formed stable colloidal dispersion in organic solvent such as chloroform, toluene, hexane, ethanol and methanol.

In Figures 8 and 9a-b optical spectra of the functionalized samples, respectively SiNP-A-ODE, SiNP-B-ODE and SiNP-B-DEC, dispersed in hexane, are reported. For SiNP-A-ODE (Figure 8), a blue shift of emission maximum respect to the as-prepared powder is recorded, but the intensity is quite low. SiNP-B-ODE (Figure 9a) and SiNP-B-DEC (Figure 9b) shows red luminescence with λ_{max}= 650 nm in both the samples. Even if spectrophotometer signals seem to be low, dispersions of functionalized nanoparticles in hexane show naked eye visible luminescence on exposition to common UV lamp (inset of Figure 9a, 9b).

Different optical properties of the powders SiNP-A and SiNP-B are probably due to different dimensions of the nanoparticles: SiNP-B have a good percentage of nanoparticles under 10 nm, and this portion of particles are probably responsible for this high luminescence. The PL properties are sensitive to the solvent, in particular in toluene and in chloroform, the PL intensity is lower, probably due to a quenching effect.

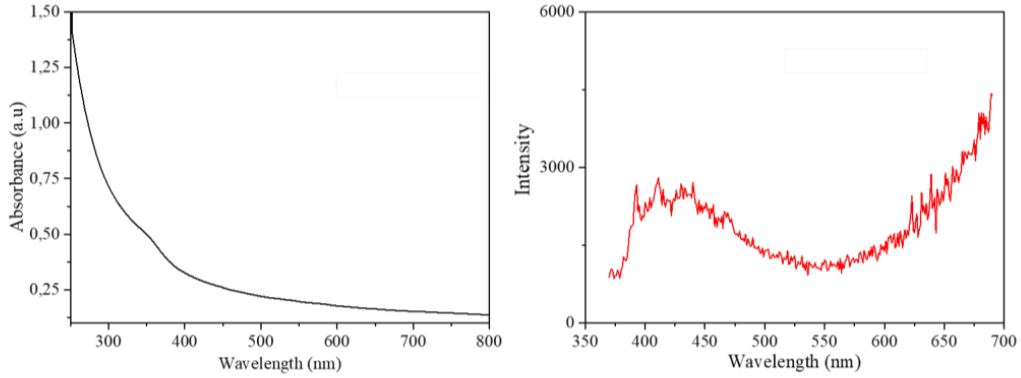

Figure 8. Absorption (a) and emission (b) spectra of sample SiNP-A-ODE in hexane.

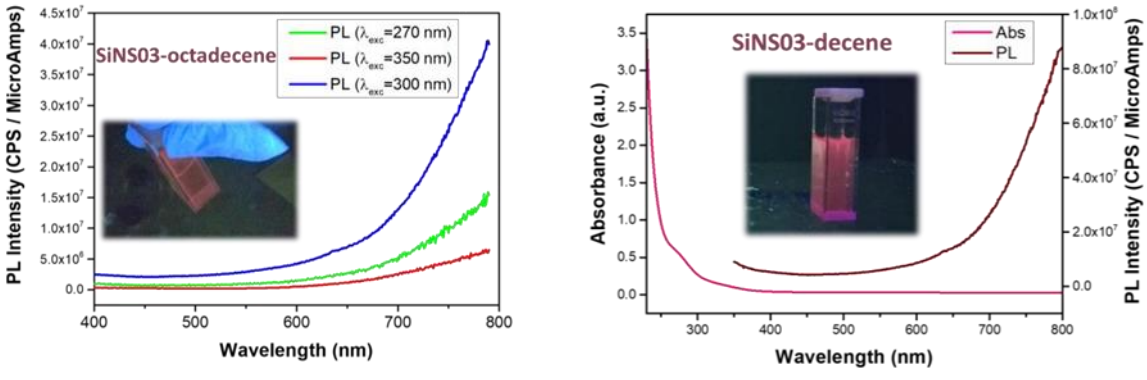

Figure 9. PL spectra of sample SiNP-B-ODE (a) and absorption and emission spectra of SINP-B-DEC (b) in hexane

7. LCA analysis

The aim of the LCA study are to identify the potential environmental impacts coming from the Si nanocrystals laser production.

Goal and scope

Goal is to evaluate the environmental burdens of the production of 100g of SiNPs with the laser pyrolysis. The function Unit is 100 g SiNPs.

The system boundary is from cradle to grave and includes the production of raw and auxiliary materials, transport, packaging and direct emission.

The main assumptions of the study are: i) the Italian electricity mix is considered because the production of SiNPs is performed in Italy; ii) the packaging is reused, so the bottle used to transport raw and auxiliary materials are not included in the study; iii) the auxiliary and raw materials are purchased near Rome, so an average transport distance of 20 km is assumed. The LCA software GaBi 6 was used for modelling and calculations. Methods ILCD Recommended Life Cycle Impact (LCI) Assessment (European Commission, 2012) was adopted as method to evaluate the environmental impacts.

Inventory phase

The result from the LCI is a compilation of the inputs (resources) and the outputs (emissions) from the product over its life cycle in relation to the functional unit. The data collection comprehends production of SiNPs and production of mix laser gases. Primary data were collected from the authors and secondary data was collected throughout commercial databases Ecoinvent 3.2.

The authors developed the laser synthesis of SiNPs, so the data used for the SiNPs production was primary data. Otherwise, the process was performed at laboratory scale and it was characterized by a production rate about 1 g/h for batch, with session of two hours and 12 hours of pumping after each session. Therefore, the energy consumption and the use of gases to prepare the product are high.

Mix laser is gaseous mixture composed by He 70%, N_2 26%, CO_2 4% v/v. The module of the laser mix considers only the amount in kg of gaseous materials, no energy consumption for the production of gases.

Energy consumption is considered for laser and pump functioning. The laser is used 2 hours for 50 times in total TL=100 h. The laser power is PL=2.5 kW so the energy consumption to produce the 100g of SiNPs is EL=250 kwh. The vacuum pump is used 24 hours for 50 times in total TP=1200 h. The pump power is PP= 2 kW. The electricity consumption for vacuum pump is Ep=2400 KWh. The total energy consumption is the sum of two contributions: E_{tot} = 2650 kWh

Raw and auxiliary materials are purchased near production location, so an average transport distance of 20 km is assumed and a Truck < 3.5 t was considered for transport. The weight of the gas tank (75 kg) used for transport of gases was included in the weight of transport. Data input for transport is 13 Kmt.

Impact analysis

Table 2 shows the Characterization Impact of the production of 100g of SiNPs.

Table 3 shows the results of characterization in percentage for each impact category. It comes out as for all impact categories the main impact is due to the Energy consumption with minimum of 68 % in “Ionising radiation” and maximum of 96% in “Freshwater eutrophication” and “Ozone depletion”, but except for “freshwater consumption”, where the main impact is due to the tap water production, owing to cooling system of laser.

These data suggest need to optimize production process to reduce energy consumption. Actually, this outcome is expected for a laboratory process, seeing as the numerous working sessions. A long-lasting synthesis surely would help to reduce energy consumption and the environmental impact of laser

synthesis. Regarding tap water consumption, the installation of a cooling plant with water recycling can improve also this impact category.

Table 2. Results of characterization

Methods	Unit	Value
Acidification, accumulated exceedance	Mole of H+ eq.	1.10E+01
Ecotoxicity for aquatic fresh water, USEtox (recommended)	CTUe	6.62E+02
Freshwater eutrophication, EUTREND model, ReCiPe	kg P eq	3.33E-03
Human toxicity cancer effects, USEtox (recommended)	CTUh	3.99E-05
Human toxicity non-canc. effects, USEtox (recommended)	CTUh	7.20E-05
Ionising radiation, human health effect model, ReCiPe	kg U235 eq	3.72E+04
IPCC global warming, excl biogenic carbon	kg CO2-Equiv.	2.07E+03
IPCC global warming, incl biogenic carbon	kg CO2-Equiv.	2.06E+03
Marine eutrophication, EUTREND model, ReCiPe	kg N-Equiv.	2.11E-01
Ozone depletion, WMO model, ReCiPe	kg CFC-11 eq	1.87E-04
Particulate matter/Respiratory inorganics, RiskPoll	kg PM2,5-Equiv.	7.25E-01
Photochemical ozone formation, LOTOS-EUROS model, ReCiPe	kg NMVOC	5.42E+00
Resource Depletion, fossil and mineral, reserve Based, CML2002	kg Sb-Equiv.	9.30E-03
Terrestrial eutrophication, accumulated exceedance	Mole of N eq.	1.83E+01
Total freshwater consumption, including rainwater, Swiss Ecoscarcity	kg	1.22E+03

8. Conclusions

In summary, CO_2 laser pyrolysis of silane in a gas flow reactor was successfully optimized to produce SiNPs apt to be functionalized with alkylic group. Relatively large quantities of powders of small particles with high degree of purity and a very dimensional distribution (about few nanometers) were collected. Deep characterization of as prepared SiNPs were performed giving insight into physical and chemical features of nanoparticles, also in relation with synthesis parameters.

We have synthesized two kinds of SiNPs covalently functionalized with 1-decene and 1-octadecene. The PL of these samples was blue-shifted, and the emission intensity was dramatically increased respect to as prepared NPs. The functionalization of the SiNPs core is an efficient strategy to tune the optical properties of SiNPs and improve their quantum efficiency.

Complementary works are necessary and in progress to better characterize the PL properties and the effect of dispersion in solvents and in polymer. In particular, dispersion of functionalized nanoparticles in polymers and deposition of these nanocomposites as films resulted in fabrication of luminescent systems that can be considered a first step for realization of Silicon-based LEDs.

Table 3. Results of characterization in percentage for each impact category.

	Mix laser RER: CO_2 liquid, at plant	Mix laser RER: He, gaseous, at plant	Mix laser RER: N_2, liquid, at plant	CH: transport, lorry 3.5-20t, fleet average	electricity, low voltage, production IT, at grid	RER: Ar, liquid, at plant	RER: C_2H_4, average, at plant	RER: SiH_4, at plant	RER: tap water, at user
Methods / Unit	0%	0%	0%	0%	96%	1%	0%	2%	0%
Acidification, accumulated exceedance/Mole of H^+eq.	0%	1%	0%	1%	94%	1%	0%	2%	1%
Ecotoxicity for aquatic fresh water, USEtox (recommended) / CTUe	0%	1%	0%	1%	91%	3%	0%	4%	1%
Freshwater eutrophication, EUTREND model, ReCiPe / kg P eq	0%	1%	0%	0%	96%	1%	0%	2%	1%
Human toxicity cancer effects, USEtox (recommended) / CTUh	0%	1%	0%	2%	92%	2%	0%	2%	1%
Human toxicity non-canc. effects, USEtox (recommended) / CTUh	0%	1%	2%	1%	68%	23%	0%	4%	2%
Ionising radiation, human health effect model, ReCiPe / kg U235 eq	0%	1%	0%	0%	92%	1%	0%	6%	0%
IPCC global warming, excl biogenic carbon/kg CO_2 eq	0%	1%	0%	0%	92%	1%	0%	6%	0%
IPCC global warming, incl biogenic carbon/kg CO_2 eq	0%	1%	0%	1%	93%	1%	0%	4%	0%
Marine eutrophication, EUTREND model, ReCiPe / kg N-Equiv.	0%	1%	0%	0%	90%	0%	0%	8%	0%
Ozone depletion, WMO model, ReCiPe/kg CFC11 eq	0%	0%	0%	0%	96%	1%	0%	2%	0%
Particulate matter /Respiratory inorganics, RiskPoll/kg PM2,5-Equiv.	0%	1%	0%	1%	92%	1%	0%	5%	0%
Photochemical ozone formation, LOTOSEUROS model, ReCiPe / kg NMVOC	0%	2%	0%	1%	94%	0%	0%	2%	0%
Resource Depletion, fossil and mineral, reserve Based, CML2002 / kg SbEquiv.	0%	2%	0%	1%	94%	0%	0%	2%	0%
Terrestrial eutrophication, accumulated exceedance / Mole of N eq.	0%	1%	0%	1%	92%	1%	0%	5%	0%
Total freshwater consumption, incl rainwater, Swiss Ecoscarcity /kg	0%	0%	0%	0%	36%	1%	0%	0%	63%

Acknowledgement
The authors wish to thank Dr. Francesco Antolini for helpful and valuable discussions on the process of nanoparticle functionalization; Dr. Antonella Lai for significant support and insight into the characterization of nanopowders with FTIR.

The described study was carried out as part of the "Nanoscrila" project implemented in the framework of the "L.R. 13/2008 - Progetti di Gruppi di Ricerca". The realization of this project is supported by the Regione Lazio (Italy).

References

[1] D V Talapin, J S Lee, M V Kovalenko, E V Shevchenko 2010 *Chem. Rev.* **110** 389-458 https://doi.org/10.1021/cr900137k
[2] X Y Cheng, S B Lowe, P J Reece, J J Gooding 2014 *Chem. Soc. Rev.* **43** 2680−2700 https://doi.org/10.1039/C3CS60353A
[3] A G Cullis, L T Canham 1991 *Nature* **353** 335−338 https://doi.org/10.1038/353335a0
[4] G Ledoux, J Gong, F Huisken, O Guillois, C Reynaud 2002 *Appl. Phys. Lett.* **80** 4834−4836 https://doi.org/10.1063/1.1485302
[5] A Gupta, M T Swihart, H Wiggers 2009 *Adv. Funct. Mater.* **19**, 696−703 https://doi.org/10.1002/adfm.200801548
[6] F J Hua, M T Swihart, E Ruckenstein 2005 *Langmuir* **21** (13) 6054−6062 https://doi.org/10.1021/la0509394
[7] B A Manhat, A L Brown, L A Black, J B Ross, K Fichter, T Vu, E Richman, A M Goforth 2011 *Chem. Mater.* **23** (9) 2407−2418 https://doi.org/10.1021/cm200270d
[8] M Dasog, Z Y Yang, S Regli, T M Atkins, A Faramus, M P Singh, E Muthuswamy, S M Kauzlarich, R D Tilley, J G C Veinot 2013 *ACS Nano* **7** (3) 2676−2685 https://doi.org/10.1021/nn4000644
[9] S Godefroo, M Hayne, M Jivanescu, A Stesmans, M Zacharias, O I Lebedev, G Van Tendeloo, V V Moshchalkov 2008 *Nat. Nanotechnol.* **3** 174−178 https://doi.org/10.1038/nnano.2008.7
[10] E Borsella, R D'Amato, F Fabbri, M Falconieri, E Trave, V Bello, G Mattei, Y Nie, D Wang 2011 *Phys. Status Solidi C* **8** 974-978 https://doi.org/10.1002/pssc.201000553
[11] M Falconieri, E Trave, R D'Amato, E Borsella 2013 *Phys. Status Solidi B* **250** (4) 831-836 https://doi.org/10.1002/pssb.201200893
[12] ISO, 2020a. ISO 14040:2006/AMD 1:2020 Environmental management — Life cycle assessment — Principles and framework — AMENDMENT 1. Geneva, Switzerland.
[13] ISO, 2020b. ISO 14044:2006/AMD 2:2020 Environmental management — Life cycle assessment — Requirements and guidelines — Amendment 2. Geneva, Switzerland
[14] S Scalbi, V Fantin, F Antolini 2017 *Journal of Cleaner Production* **142** 3702–3718 https://doi.org/10.1016/j.jclepro.2016.10.098
[15] R D'Amato, M Falconieri, F Fabbri, V Bello, E Borsella 2010 *J. Nanopart. Res.* **12** 1845-1858 DOI 10.1007/s11051-009-9746-3.
[16] C M Hessel, E J Henderson, J G C Veinot 2006 Chem. Mater. 18 (26) 6139−6146 https://doi.org/10.1021/cm0602803
[17] J M Buriak 2002 *Chem. Rev.* **102** (5) 1271−1308 https://doi.org/10.1021/cr000064s
[18] I H Campbell, P M Fauchet 1986 *Solid State Commun.* **58** (10) 739-741 https://doi.org/10.1016/0038-1098(86)90513-2
[19] R L C Vink, G T Barkema, W F van der Weg 2001 *Phys. Rev. B* **63** (11-15) 115210 https://doi.org/10.1103/PhysRevB.63.115210
[20] F J Himpsel, F R McFeely, A Taleb-Ibrahimi, J A Yarmoff 1988 *Phys. Rev. B* **38** (9-15) 6084-6096 https://doi.org/10.1103/PhysRevB.38.6084